Sensitivity of the seismic response of monopile-supported offshore wind turbines to soil variability

Panagoulias, S.; de Winter, C.; Navalkar, S. T.; Nernheim, A.

DOI
10.1016/j.oceaneng.2022.113545

Publication date
2023

Document Version
Final published version

Published in
Ocean Engineering

Ocean Engineering 268 (2023) 113545

Contents lists available at ScienceDirect

Ocean Engineering

journal homepage: www.elsevier.com/locate/oceaneng

Sensitivity of the seismic response of monopile-supported offshore wind turbines to soil variability

S. Panagoulias [a,b,*], C. de Winter [b], S.T. Navalkar [a,b], A. Nernheim [c]

[a] Delft University of Technology, Mekelweg 5, Delft, 2628 CD, The Netherlands
[b] Siemens Gamesa Renewable Energy, Pr. Beatrixlaan 800, The Hague, 2595 BN, The Netherlands
[c] Siemens Gamesa Renewable Energy, Beim Strohhause 17-31, Hamburg, 20097, Germany

ARTICLE INFO

Keywords:
Offshore wind turbine
Monopile foundation
Earthquake loading
Seismic design
Soil–structure interaction
Probabilistic analysis
Numerical analysis

ABSTRACT

The expansion of the offshore wind industry in areas with high seismicity has led to engineering challenges related to the design of the offshore wind turbines (OWTs). Monopiles, i.e., tubular steel piles of large outer diameter, low aspect ratio (penetration depth over outer diameter), and relatively thin pile wall, are traditionally the preferred foundation type for OWT due to fabrication, transportation, and installation standardization. For all bottom-founded systems, soil–structure interaction (SSI) plays a crucial role in the system's response. Additional challenges arise in the case of seismic SSI as, not only the system's response, but also the seismic ground motion itself are affected by the soil characteristics. Furthermore, uncertainties related to soil properties, as derived from the soil testing campaign and interpretation, need to be thoroughly considered for OWT load calculations and the design of the support structure. The uncertainty in soil interpretation may have a large impact on the characteristics of the input seismic motion. Subsequently, SSI will affect the seismic loads acting on the support structure and the OWT. This knock-on effect of the interpretation of the soil parameters is unknown, but may be significant to account for. In fact, when a "best estimate" soil parameter set is used, the resulting seismic load may not necessarily correspond to the most probable load for the assumed seismic event. This paper investigates the influence of the uncertainty in soil parameters, as they may result from the soil interpretation, on the seismic loads. It demonstrates the skewed distribution of OWT seismic loads using a realistic design case study on a commercial OWT. Results are presented in the form of transfer functions, response spectra at mudline and normalized bending moments along the support structure. Three distinct structural components of interest are selected to evaluate the results. It is concluded that, for the analysis of OWT under seismic loading conditions in particular, it cannot be decided a priori which soil properties would result in conservative or progressive design. Based on the obtained results, recommendations are given which aim to de-risk and enhance the current design practice.

1. Introduction

The rapid growth of the offshore wind industry in regions such as the United States and the Asia–Pacific (APAC), is following the global demand of renewable energy towards a more sustainable, low-carbon future (GWEC, 2022). Natural phenomena such as earthquakes, tsunamis and cyclones are imposing unprecedented engineering challenges on the offshore wind developments and, in particular, the design of offshore wind turbines. Ashford et al. (2011) provide evidence of how strong earthquakes may severely impact wind turbine support structures.

Monopiles (MP), i.e., tubular steel piles of large outer diameter (>5 m), low aspect ratio between penetration depth and outer diameter (2–6), and relatively thin pile wall (≈D/100), are traditionally the preferred foundation type for bottom-founded offshore wind turbines (OWT). This is due to fabrication, transportation, and installation standardization needed to meet the tight timelines and budget constraints necessary to achieve economic feasibility of offshore wind power plants.

Fig. 1 illustrates a typical support structure configuration for a MP-founded OWT (modified after Page et al. (2018)). Conventionally, the transition piece together with the monopile constitute the foundation of the structure, being under the responsibility of the Foundation

* Corresponding author at: Delft University of Technology, Mekelweg 5, Delft, 2628 CD, The Netherlands.
E-mail addresses: s.panagoulias@tudelft.nl, stavros.panagoulias@siemensgamesa.com (S. Panagoulias), corine.dewinter@siemensgamesa.com (C. de Winter), sachin.navalkar@siemensgamesa.com (S. Navalkar), axel.nernheim@siemensgamesa.com (A. Nernheim).

https://doi.org/10.1016/j.oceaneng.2022.113545
Received 30 June 2022; Received in revised form 7 October 2022; Accepted 22 December 2022
Available online 4 January 2023

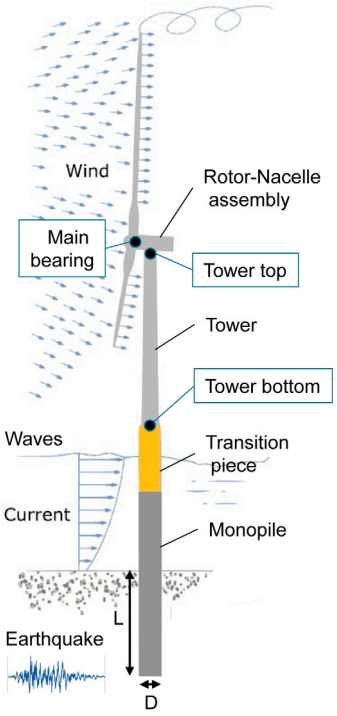

Fig. 1. Components of OWT support structure with main acting environmental and seismic loads. Three distinct structural components are also depicted, which will be used to evaluate the obtained results.
Source: Modified after Page et al. (2018).

Designer. The tower and the rotor-nacelle assembly (RNA) fall under the scope of the Wind Turbine Manufacturer. In the same figure, the various environmental loads (wind, wave, current) and the earthquake loads are also simplistically depicted. In addition, the location of three main structural components, which will be used to analyse the results of this study, is highlighted: main bearing, tower top and tower bottom. Note that the tower bottom is also the interface point between the tower and the foundation in line with the typical split scope discussed above, and thereby, a location of high interest for the involved design parties.

The seismic response of shallow-founded (e.g. footings) and embedded structures (e.g. slender piles) has been studied extensively by many researchers over the past years (for instance: Matlock et al. (1978), Gazetas et al. (1995) and Hussien et al. (2015)). However the particular characteristics of the MP-supported OWT, mainly in relation to the geometrical properties of the foundation, the low system damping and the narrow window of design/targeted eigenfrequencies for best performance and low fatigue damage over lifetime, lead to various design challenges. As indicated by other researchers (Katsanos et al., 2016; Kaynia, 2019; Bhattacharya et al., 2022), there are various considerations with respect to the design of OWT against seismic loading. The recently released DNV-RP-0585 (2021) is paving the way for a better-established seismic design practice for OWT.

Soil–structure interaction (SSI) plays a crucial role in the static and dynamic response of all such bottom-founded systems (Kausel, 2010; Medina et al., 2013; Pisanò, 2019). The impact of SSI on the seismic response of OWT can be studied using models of varying levels of fidelity and complexity. For a full seismic load evaluation of the blades, the RNA and the support structure, via an aero-servo-hydro-elastic simulation environment, it is common to limit the geotechnical complexity of the model. In such a case, SSI is captured with distributed lateral soil reaction curves, the so-called "p-y" curves (API, 2014).

According to Design Standards, the geotechnical and structural design needs to satisfy the Ultimate (ULS), Serviceability (SLS) and Fatigue (FLS), and Accidental (ALS) limit states (DNV-RP-0585, 2021). Uncertainty in soil parameters, due to local variation of the soil properties (aleatory uncertainty) and testing or modelling inaccuracy (epistemic uncertainty), is captured by using statistical models. These models result in soil parameters sets, such as, but not limited to, "best estimate" (hereafter BE), "lower bound" or "cautious estimate" (hereafter CE), and "upper bound" or "optimistic estimate" (hereafter OE). Each set is associated with a certain probability of exceedance or quantile of the employed probability distribution. Typically, each limit state is assessed with a certain soil parameter set, depending on the application, the design criteria, and the accepted probability of failure.

With respect to the design under seismic loading, it cannot be a priori decided which soil parameter set would result in a conservative or progressive design. The seismic excitation under consideration may be derived via site-specific Probabilistic or Deterministic Seismic Hazard Analysis (PSHA or DSHA), as described by DNV-RP-0585 (2021). However, the uncertainty in the soil properties may still lead to a broad range of seismic motion characteristics (amplitude, frequency content etc.) under free-field conditions (Tran et al., 2020). Subsequently, SSI will affect the seismic loads acting on the OWT. This knock-on effect of the interpretation of the soil parameters is unknown, but may be significant to account for. In fact, when a BE soil parameter set is used, the resulting seismic loading may not necessarily correspond to the most probable value of loads for the assumed seismic event.

To the best of the authors' knowledge, while the influence of geotechnical uncertainty on the design of MP-supported OWT has received some attention (Carswell et al., 2015; Yeter et al., 2019; Reale et al., 2021; Hsu et al., 2022), there is limited research about the influence of soil parameter variability on the seismic loads acting upon OWT. In such a loading scenario, not only the system's response, but also the seismic excitation is affected by the soil characteristics. The frequency content and the amplitude of the seismic load acting upon the foundation depends on local site effects. Uncertainties related to the engineering soil properties, as derived from the soil testing campaign and interpretation, both in-situ (e.g., via Cone Penetration Testing (CPT)) and in the laboratory (e.g., via static and cyclic triaxial and direct shear tests), need to be thoroughly considered for OWT seismic load calculations, and the design of the support structure. It is noted that the focus of the present study is on the relative effect of the adopted soil properties on the seismic response of the support structure, rather than how different soil interpretation strategies and methods could influence the values of the employed soil parameters.

Furthermore, it is broadly recognized that in regions of high seismicity, with relatively shallow and clean sand deposits, liquefaction may impose design risks and engineering challenges (Bhattacharya et al., 2021; Patra et al., 2022; Zhang et al., 2022). Despite the crucial impact that liquefaction may have on the response of OWT under seismic loading, the present study neglects this effect, and focuses on the objectives presented above. The findings are still valid for cases of non-liquefiable soil deposits and weak to moderate seismic loading. The results of the current investigation may be extrapolated to the additional uncertainty introduced by liquefaction of soils. However, such extrapolation is not considered to be within scope of the present study.

This paper investigates the impact of geotechnical uncertainty, in the form of varying soil properties, on the seismic loading of OWT. The aim is to de-risk and enhance the current design practice. The study is based on input data which are representative of a typical offshore wind project in the APAC region. Section 2 provides information regarding the applied methodology and related assumptions, while Section 3 gives insight into the considered input parameters and modelling configuration. Sections 4 and 5 present and discuss the obtained results. Section 6 summarizes the key findings, including recommendations related to the seismic design of OWT, and suggestions for further research.

2. Methodology

Uncertainties related to the soil properties may have a direct effect on the profiles of soil strength and stiffness used for the design of OWTs. The adopted soil profile will influence the dynamic response of the OWT not only by affecting the system's eigenfrequencies and its lateral response, but also by modifying the earthquake signal that is being propagated through the soil, and is eventually acting upon the structure. The methodology outlined below is followed to address quantitatively the objective of this study as presented in Section 1. It is also noted that the employed methodology is based on the methodology followed in the ACE (Alleviating Cyclone and Earthquake Challenges for Wind farms) Joint Industry Project (ACE JIP, 2021), led by DNV. The project resulted in the publicly released DNV-RP-0585 (2021). To reach ACE's objectives, different wind turbine analysis and design software (e.g., SGRE's BHawC, DNV's Bladed) were used for cross-verification and comparison of results. An elaborate report was produced by DNV and distributed among the project partners (DNV, 2021).

For the case study considered in this paper, a BE soil interpretation is established representing the "reference" soil profile. Based on that, the CE and OE soil profiles are derived which are used as additional "reference" cases, in line with the discussion in Section 1. Moreover, based on the BE soil interpretation, additional soil profiles are generated with soil properties which vary following probabilistic distributions. The lateral soil reaction curves are also calibrated for each generated soil profile. Further information is presented in Section 2.1.

Different seismic input motions are considered to study the effects under different seismic characteristics. Relevant information is provided in Section 2.2. Under the assumption of vertically propagating shear waves, one-dimensional site response analyses are used to derive seismic accelerations along the soil profiles. Section 2.3 presents the underlying methodology.

Assumptions related to the operational state of the OWT and the environmental loading conditions are based on design experience and selected such that a conservative numerical modelling approach is adopted. The input to the different components of the numerical simulations is discussed in Section 3.

2.1. Soil properties and soil reaction curves

The soil properties corresponding to the BE soil interpretation are established via in-situ and laboratory testing data that can be obtained for a representative project location, at a seismically active region in APAC. Table 1 presents the BE soil properties.

Besides the BE soil profile, the CE and OE soil profiles are also defined as "reference" cases (see Section 1). Based on design experience, the values of the strength and stiffness soil properties, related to the CE and OE soil interpretations, are chosen to vary from the corresponding BE values within a range of ±50% of one standard deviation. The latter equals 25% of the BE (mean) value.

Additionally, one hundred (100) different soil profiles are generated by modifying the BE soil parameters as described below. The "random" generation algorithm of MATLAB (2018) is used to produce the soil parameters variation, following a Monte Carlo simulation approach for sensitivity investigation.

- In line with DNV-RP-C207 (2015) the small-strain stiffness (G_{max}), and therefore the shear wave velocity (v_s), the internal friction angle (ϕ') and the undrained shear strength (s_u) follow a Gaussian distribution with mean value equal to the BE value per soil layer as presented in Table 1, and a standard deviation equal to 25% of that mean value. The assumed standard deviation originates from practical experience with various offshore wind projects around the globe. Indicatively, Fig. 2(a) illustrates a histogram graphical representation of G_{max} per soil layer. It is visible that the employed random generation algorithm does not create "perfect" normally distributed profiles within the one hundred realizations. Such deviation from an "ideal" Gaussian distribution is regarded as acceptable by the authors, as it sufficiently generates the desired variation in the soil properties. Fig. 2(b) depicts the variation of G_{max} over depth. For comparison, the soil profiles which correspond to the BE, CE and OE interpretations are also presented in the plot.
- The saturated soil density ρ, and the plasticity index (PI) of the clay soil layers, are assumed to follow a uniform distribution, implying that these soil parameters are not altered throughout the numerical analyses. This assumption allows to solely study the impact of soil strength and stiffness variations on the seismic load. However, it is acknowledged that PI has a significant impact on the stiffness modulus reduction and damping curves of clayey materials. Thus its effect is being investigated separately by assigning three different PI values to the clay layers of the BE soil profile. The results of this separate study are presented in Section 4.

The distributed lateral soil reaction curves are calibrated to reflect the properties of each one of the adopted soil profiles. At first, the soil reaction curves for the BE soil profile are generated according to SGRE's in-house developed methods. The applied formulation is an enhanced version of the classical p-y approach for lateral-only non-linear soil springs (API, 2014; Jeanjean, 2009), mainly in relation to the small-strain stiffness, aiming to capture soil reaction in case of laterally loaded monopiles. Specifically for sand soil layers (API, 2014), the ultimate capacity of the reaction is controlled by the internal friction angle (ϕ'), while the initial stiffness and the curvature are adapted using the small strain shear modulus (G_{max}). For clay soil layers, the employed formulation is based on Jeanjean (2009); the ultimate capacity is controlled by the undrained shear strength (s_u) and the selected failure mechanism (via the parameter N_p), while the small strain shear modulus (G_{max}) affects the initial stiffness and the curvature of the soil reaction curve. Further information is deemed confidential at the moment of writing this article.

After having calibrated the curves for the BE soil profile, the variation of the soil parameters, as described above, is used as input to the soil reaction curves formulation. This procedure allows for generation of multiple sets of soil reactions in a quick and robust manner.

It may be noted that, while latest research indicates that additional soil reaction components may be needed to accurately capture the MP lateral response (Byrne et al., 2019; Panagoulias et al., 2020; Wang and Ishihara, 2022), the adopted modelling strategy is considered adequate in relation to the objective of the present study.

Furthermore, as literature suggests, intense seismic loading may compromise the serviceability design requirements via accumulation of rotation and/or settlement (Gelagoti et al., 2019; Kaynia, 2019). This phenomenon might be intensified in case of soil liquefaction (Anastasopoulos and Theofilou, 2016). It is acknowledged that the employed non-linear elastic soil reaction curves cannot provide insight into such post-seismic accumulated deformations.

2.2. Seismic motions

Four different seismic motions have been selected from the standard input suite of the software *ProShake* (EduPro Civil Systems, 2020). The adopted code names and the main characteristics of each motion are summarized below and in Table 2.

One seismic motion is selected from the M_w 6.9 El Centro earthquake which occurred on May 18, 1940, at the San Joaquin Valley in Southern California. One seismic motion is chosen from the M_w 7.5 Kern Country earthquake which occurred on July 21, 1952, on the strike-slip fault White Wolf, located at the San Joaquin Valley in Southern California. Two seismic motions are selected from the M_w

Table 1
Soil properties corresponding to the BE soil interpretation.

Soil type	Top depth (m)	Thickness (m)	ρ (t/m^3)	ϕ' (°)	s_u (kPa)	PI (%)	v_s (m/s)	G_{max} (MPa)
Sand	0.0	3.0	1.83	35	–	–	130	33
Sand	3.0	2.0	1.83	40	–	–	150	43
Clay	5.0	5.0	1.68	–	70	30	110	21
Clay	10.0	5.0	1.68	–	80	30	130	30
Sand	15.0	10.0	1.89	40	–	–	250	117
Sand	25.0	25.0	1.89	37	–	–	310	178
Sand	50.0	10.0	1.89	35	–	–	370	256
Sand	60.0	10.0	1.89	33	–	–	400	301
Clay	70.0	10.0	1.89	–	350	30	425	340

ρ: saturated soil density; ϕ': internal friction angle; s_u: undrained shear strength; PI: plasticity index; v_s: shear wave velocity; G_{max}: small-strain shear stiffness.

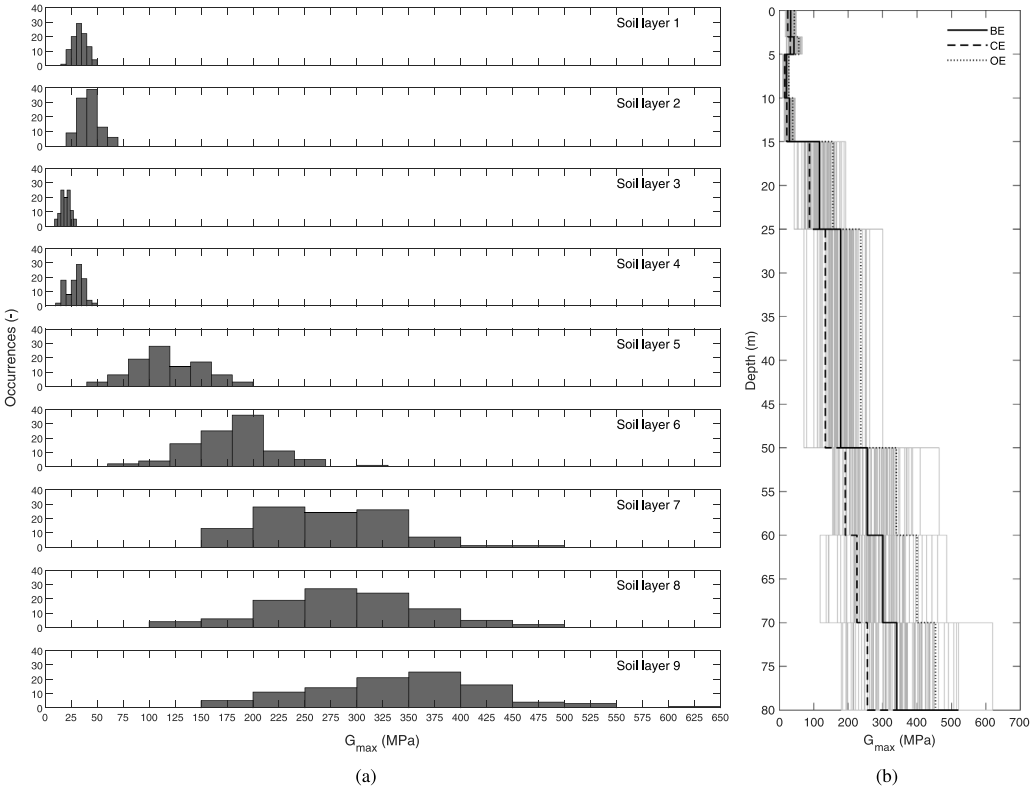

(a) (b)

Fig. 2. Histogram of the adopted values of G_{max} per soil layer, per simulation (one hundred occurrences in total) and the corresponding variation of G_{max} over depth.

6.9 Loma Prieta (Santa Cruz Mountains) earthquake which took place on October 17, 1989, with an epicentre about 14 km northeast of Santa Cruz and 96 km south-southeast of San Francisco. Both of them represent far-field rock-input records (Borcherdt, 1994).

- "El Centro": El Centro station, Imperial Valley Irrigation District (horizontal component 180).
- "TAFT": TAFT Kern County station, CA - Lincoln School (horizontal component 111).
- "Loma Prieta - DH": Loma Prieta, station Diamond Heights (horizontal component 90).
- "Loma Prieta - YBI": Loma Prieta, station Yerba Buena Island (horizontal component 90).

The acceleration time series of the four seismic motions are illustrated in Fig. 3(a), while Fig. 3(b) presents the corresponding spectral accelerations. Note that only the "Loma Prieta" motions represent rock-input records, while the "El Centro" and "TAFT" motions are recorded on alluvium deposits, therefore, not representing true free-field outcrop recordings. However, the selection of the employed input motions is based on two main criteria: the rich frequency content (which is covering higher fundamental modes of the system) and variation in the accelerations amplitude. Owing to confidentiality, the exact seismic motions corresponding to the offshore site that the present study was based on could not be used. Derivation of more accurate seismic motions based on the seismic characteristics of a representative location in a seismically-active region, e.g., via Probabilistic Seismic Hazard Analysis (PSHA), and scaling or spectral matching to conform with International or National Design Standards, is deemed unnecessary,

Table 2
Main characteristics of the employed seismic motions.

Seismic motion	PGA (m/s^2)	$S_{a,1\ Hz}$ (m/s^2)	T_p (s)	f_{mean} (Hz)
El Centro	3.37	4.98	0.68	6.20
TAFT	1.81	1.57	0.33	4.74
Loma Prieta - DH	1.11	1.34	0.41	4.32
Loma Prieta - YBI	0.66	0.71	1.41	4.64

PGA: peak ground acceleration; $S_{a,1\ Hz}$: spectral acceleration at 1 Hz; T_p: predominant period (estimated based on the maximum amplitude of the raw Fourier spectrum); f_{mean}: mean frequency.

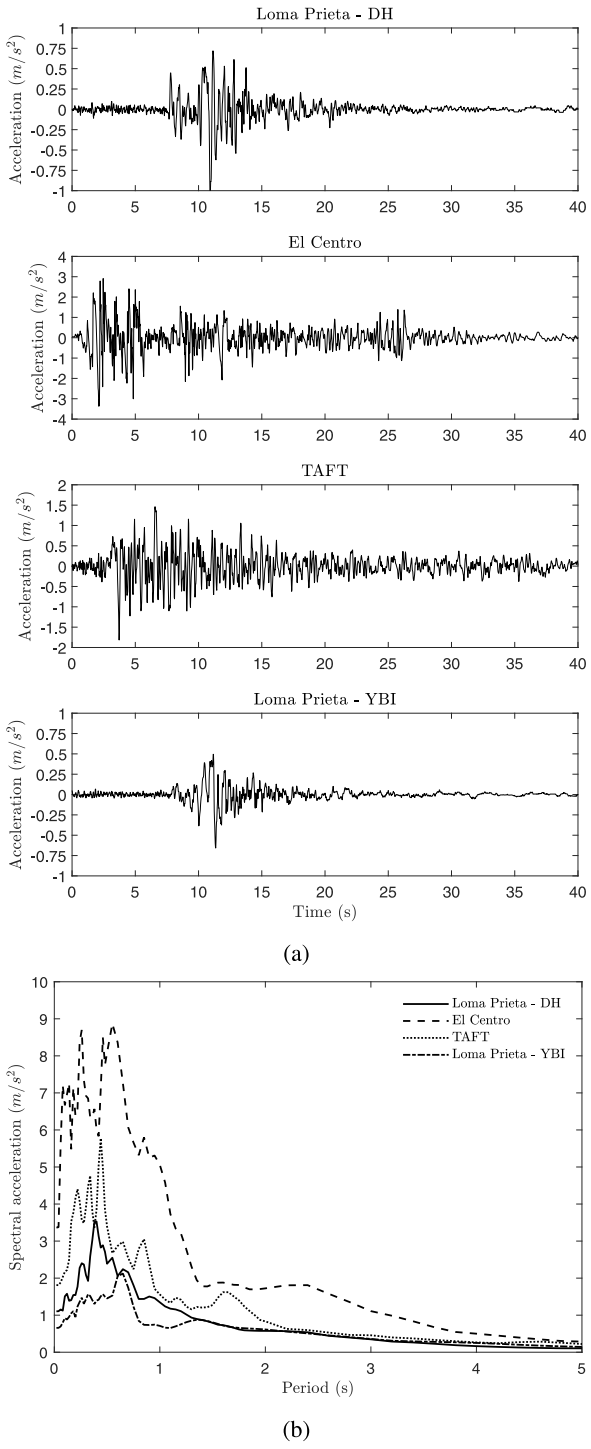

Fig. 3. Acceleration time series (a) and spectral acceleration of the four earthquake motions used in this study (b).

because the selected seismic motions are being used as indicative motions to investigate the research objectives discussed in Section 1.

2.3. Site response analysis

One-dimensional (1D) site response analysis (SRA) is conducted with the program *ProShake* (EduPro Civil Systems, 2020). Frequency-domain equivalent-linear simulations are employed to compute the earthquake excitation signals along depth at free-field for the four selected input seismic motions presented in Section 2.2. The seismic motion is applied as "outcrop motion", representing a signal that was recorded at free surface. Shear stiffness modulus reduction and damping curves are modelled after Seed and Idriss (1970) for sand layers, and Vucetic and Dobry (1991) for clay layers. Bedrock is modelled assuming a soft rock formation of unit weight equal to 20.4 kN/m^3 and shear wave velocity of 500 m/s laying below the soil profile, i.e., at 80 m depth. This assumption is deemed realistic as it is based on the stratigraphy of the offshore site under consideration.

The modelling of the non-linear and inelastic soil response via an equivalent linear approach is an acceptable simplification in earthquake engineering as long as the induced soil non-linearity remains relatively low, i.e., for moderately stiff soil profiles and relatively weak seismic motions (Kramer, 1996). The authors trust the acceptance of the equivalent linear method for the conditions analysed in the present study. This is further discussed in Section 6.

3. Numerical simulations

The impact of the variability of soil properties on the wind turbine load response to seismic events is investigated using the aero-servo-elastic simulation environment BHawC (Bonus Horizontal axis wind turbine Code), described in Rubak and Petersen (2005). The fully nonlinear, time-domain simulation environment BHawC has been used extensively for more than 17 years for the design and development of onshore and offshore utility-scale wind turbines of Siemens Gamesa Renewable Energy (SGRE). BHawC has been validated in terms of power performance and load measurements in the field using full-scale prototype wind turbines. Guntur et al. (2017) made use of experimental measurements obtained from a megawatt-scale SGRE wind turbine located at the National Renewable Energy Laboratory (NREL) in the USA. This turbine was instrumented with blade sensors, surface-pressure taps, and strain gauges for support structure load measurements. The same turbine was modelled in BHawC and subjected to the same environmental/wind conditions as experienced by the prototype. The one-to-one comparison was performed in time-domain, at the level of ten-minute statistics, but also in the frequency-domain. A successful validation was reported with respect to the turbine operation (in terms of power, speed and pitch) and the measured loads (including rotor thrust, blade deflection and tower bending moments). Therefore, sufficient correspondence was achieved between simulations and measurements to certify the use of BHawC for turbine design and load evaluation.

The structural model in BHawC includes fully flexible blades, nacelle elements, tower and foundation. The flowchart depicted in Fig. 4 presents the connection and interaction between the various components. For the current study, the turbine is modelled as an offshore turbine with a monopile foundation. As an aeroelastic simulation environment, BHawC affords the user the possibility to define the aerodynamic behaviour of the blades using two-dimensional lift, drag and moment polars. Normal turbine operation can be commanded via a controller DLL (dynamic link library) file, identical to the one used in full-scale turbines, that communicates at each control time step with the BHawC environment and provides the necessary actuator inputs. For the current study, a model setup of the commercial offshore wind turbine *SG-DD-167* of SGRE has been used to perform the seismic simulations. The specifications of this turbine, as used for this study, are given in Table 3. The properties of the employed support structure are presented in Table 4.

Since the purpose of the current study is to evaluate the seismic response of the turbine, a few modifications are done to the typical BHawC simulation setup. To gain good understanding of the sensitivity of soil parameters to the structural response and loads, the impact of confounding factors arising out of aerodynamics, hydrodynamics and the controller has been considered out of the current scope, while retaining a realistic model setup as described below.

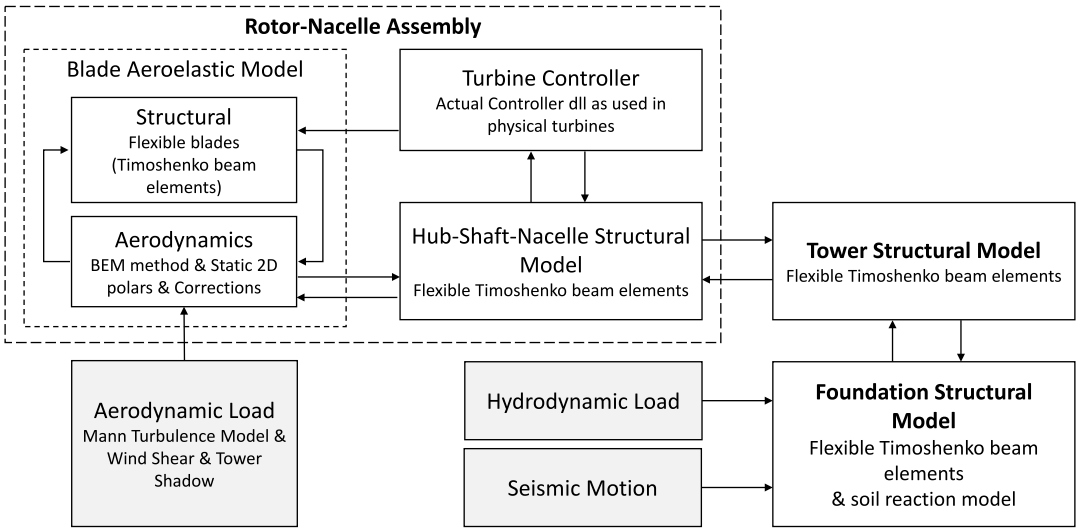

Fig. 4. Flowchart of the BHawC components.

Table 3
SG-DD-167 Wind turbine setup specifications.

Description	Symbol	Value
Rated power	P_{rated}	8.6 MW
Rotor diameter	d_{ro}	167 m
Cut-in wind speed	v_{cutin}	3 m/s
Rated wind speed	v_{rated}	14 m/s
Cut-out wind speed	v_{cutout}	25 m/s
Gearbox ratio	ν	1.0 [Direct-Drive]

Table 4
Support structure specifications; mLAT indicates distance from the Lowest Astronomical Tide in m, which is the adopted zero level.

Description	Symbol	Value
Hub height elevation	H_{hub}	113 mLAT
Transition piece elevation	H_{TP}	22 mLAT
Mudline elevation	H_{mud}	−26 mLAT
Pile-tip elevation	H_{PT}	−62 mLAT
Pile penetration depth	L	36 m
Pile diameter (outer)	D	7.5 m

In line with recently published research findings (Alati et al., 2015; Patra and Haldar, 2021), SGRE's design experience in seismic projects indicates that a turbine under normal operation will show lower loads than a turbine at standstill, under moderate to strong seismic loading (Xi et al., 2021, 2022). This is due to the presence of aerodynamic damping arising out of the rotor's spinning (Valamanesh and Myers, 2014; Liu et al., 2017). Operational loads, including transient loads during turbine shutdown, even if combined with the seismic loads, are typically less severe than the design-driving seismic loads seen when a turbine is at standstill. Therefore, the present study focuses on an OWT at idling state (Design Load Case (DLC) 11.3 of DNV-ST-0437 (2016)). However, it is noted that power production, (emergency) shutdown and idling conditions should be evaluated for the design of OWTs under seismic loading (IEC61400-3, 2019), as the observations above are not reported as conclusive design recommendations, but rather to support the BHawC simulation setup adopted for this study. Potential adverse effects of seismic directionality are also acknowledged (Mo et al., 2021), but they are not considered in the present study (see the "Seismic motion" assumptions presented below).

- **Turbine Controller**: The turbine is simulated at standstill, so the controller is not active.
- **Aerodynamic Load**: The aerodynamic module of BHawC has been disabled, and dynamic loading of the turbine due to environmental turbulence is not present in the results presented in this paper. User experience has shown that seismic events that cause design-driving turbine loads are typically significantly higher than the contemporaneous turbulent wind-induced dynamic loads. As such, the load evaluation is not materially affected by the lack of wind-induced aerodynamic loading.
- **Aerodynamic Damping**: Aerodynamic damping, typically arising out of the ambient wind speed, but also out of turbine fore-aft motion, is no longer present in the simulation results presented in this paper as the aerodynamic module has been disabled. As a direct consequence of the lack of this source of damping, seismic load responses presented are higher than what may be expected in the field.
- **Hydrodynamic Load**: While the turbine is modelled as an offshore turbine, hydrodynamic wave loads have been disabled in the simulations of this study. Hydrodynamic loads corresponding to a normal sea state are typically less severe than design-driving seismic loads for key structural components.
- **Damping formulation**: The system's total damping, representing all different background damping components (soil, hydrodynamic, structural and aerodynamic), and passive damping devices (i.e., dampers placed in the tower), is applied via the Rayleigh damping formulation. The employed non-linear elastic soil reaction curves (see Section 2.1) do not provide additional soil material damping. The Rayleigh parameters are set such that the damping for the first and second eigenmodes is equal to 2.5% and 6.0% logarithmic decrement (0.4% and 0.95% critical damping) respectively.
- **Soil profiles**: As discussed in Section 2.1, the values of the soil properties per layer vary such that a normal distribution is fitted to the employed soil profiles.
- **Seismic Motion**: Four seismic input motions, as presented in Section 2.2, are employed in this study. The seismic signal is applied horizontally at the bottom of each varying soil profile (Section 2.1), while 1D SRA is used to derive the seismic signal over depth, under the assumption of vertically propagating shear waves (Section 2.3). The derived seismic motions are applied at the "free" end of the soil reaction curves along the monopile, from mudline to pile tip. Only one seismic direction is analysed in the present study, which is the fore-aft (FA) direction of the turbine, so that the imposed seismic motion is perpendicular to the rotor plane. Design experience has shown that seismic loading

Table 5
System's eigenfrequencies ($f_{n,x}$) in the fore-aft (FA) and side-side (SS) directions for three different soil interpretations (BE, CE and OE).

Soil interpretation	BE	CE	OE
$f_{1,FA}$ (Hz)	0.205	0.201	0.208
$f_{1,SS}$ (Hz)	0.209	0.205	0.212
$f_{2,FA}$ (Hz)	0.885	0.842	0.924
$f_{2,SS}$ (Hz)	0.922	0.876	0.963

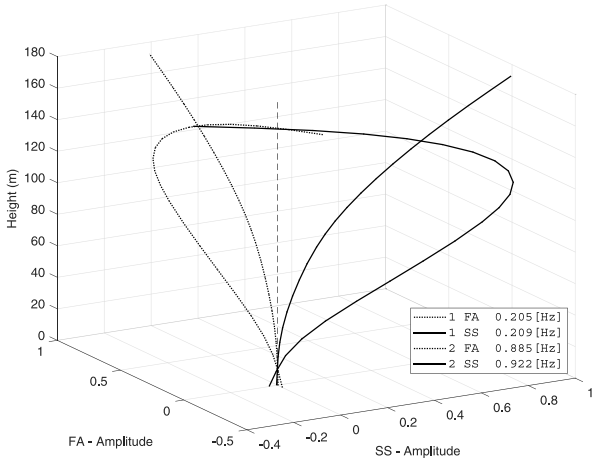

Fig. 5. System's eigenmodes and eigenfrequencies in the fore-aft (FA) and side-side (SS) directions for the BE soil interpretation.

applied to this direction results in the highest loads for several key structural components. The phenomena studied in this paper are also expected to be amenable to extrapolation to other directions of seismic loading.

Based on the information above, the baseline simulation setup considered in this study corresponds closely to OWT in standstill (idling condition) subjected to a severe seismic event, occurring predominantly in the fore-aft direction, where the environmental conditions correspond to very low wind speeds and a calm sea state.

In Table 5 the impact of the variation of the soil material parameters on the system's eigenfrequency can be found. The values of the 1st and 2nd eigenfrequencies are presented for the three distinct soil interpretations, namely BE, CE and OE. Both fore-aft (FA) and side-side (SS) directions are presented. As discussed further above the seismic signal is applied to the FA direction, but both FA and SS are hereby presented for completeness. The stiffer the soil profile (i.e., OE), the higher then eigenfrequency of the system. Fig. 5 illustrates the corresponding eigenmodes. The presented values do not cover the full employed variability of soil properties as discussed in Section 2.2. They are bounded by CE and OE soil interpretations. This simplification is considered adequate to draw meaningful conclusions. The 3rd eigenmode is not presented as, being highly damped, is not dominating the seismic response in this study.

4. Results

The results of the numerical analyses, with the setup presented in the previous Sections, are presented below.

Fig. 6 shows the impact of the plasticity index (PI), which is assigned to the clay layers, on the transfer functions from bedrock to mudline. Three different cases are analysed with PI equal to 15, 30 and 45. The BE soil profile is used. All other soil parameters remain unchanged. For this study only one seismic motion is considered, the "Loma Prieta - DH". This figure shows that any uncertainty associated with the values of the PI values has a considerable impact to the amplitude and

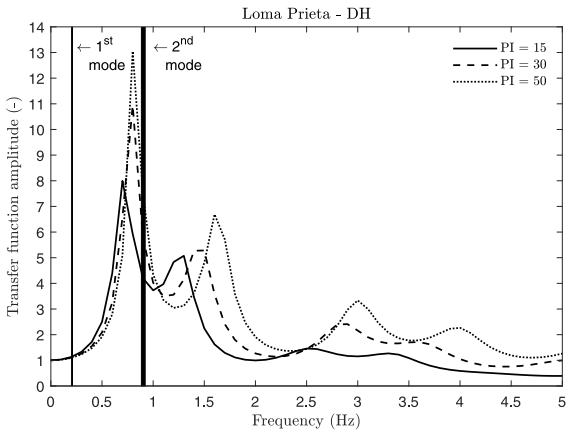

Fig. 6. Transfer functions (bedrock to mudline) for different plasticity indices (PI) of the clay layers. All other material parameters correspond to the BE soil interpretation. The imposed seismic motion is the "Loma Prieta - DH".

frequency content of the transfer functions. A higher PI would lead to stiffer soil response, shifting the frequency content towards higher values, and less soil damping. In the presented case, an increase of PI will most probably lead to higher loads as the shifted amplitude peak gets closer to the 2nd eigenmode of the support structure.

Fig. 7 illustrates the obtained amplitude of the transfer functions between bedrock and mudline, after imposing the four different earthquake motions to the one hundred randomly generated soil profiles. The results correspond to the free-field seismic motion. The three reference soil interpretations, i.e., the BE, CE and OE, are also highlighted with distinct lines. The CE soil interpretation, which corresponds to a "soft" soil profile has amplitude peaks which are consistently at lower frequencies comparing to the BE soil interpretation. The opposite is true for the OE soil interpretation. Moreover the OE results indicate that the OE soil interpretation is stiffer than the stiffest of the one hundred soil profiles. This is caused by the randomness algorithm for the generation of the one hundred soil profiles. While it is true that a higher number of profiles would eventually lead to finer normally distributed values of the soil properties, the authors consider the number of the generated profiles adequate to draw meaningful conclusions.

In the same figure the ranges of the 1st and 2nd eigenmodes are also presented (see Table 5). In all four earthquakes, the 2nd eigenmode is at the vicinity of the maximum amplitude, while the 1st mode is located at lower frequencies where the amplitude is about one. This is an indication that the 2nd eigenmode will be governing the response of the support structure. The 3rd eigenmode is not presented because its frequency and the associated total damping are higher, eventually not leading to critical loading.

While an increasing trend in the amplitude of the transfer function peaks with increasing soil stiffness is observed (i.e., OE peaks tend to be higher than BE), it should be noted that resonance of soil's response with the system's eigenfrequencies is far more critical for the structural loading.

Fig. 7 also indicates that the "El Centro" seismic motion, which is the one with the highest spectral energy content throughout the entire range of frequencies (or periods; see Fig. 3(b)), appears to have the smallest amplitude of transfer functions. This is possibly related to the high accelerations of "El Centro", which generate high effective shear strains along the soil profile. Higher strains have a dual effect on the response. Firstly, they lead to higher soil damping values. Secondly, they result in smaller "equivalent linear" stiffness (see Section 2.3), which might trigger softer soil response, and therefore "de-amplification" of the higher frequency content of the motion. As indicated in Table 2, "El Centro" has the highest mean frequency of the four considered motions.

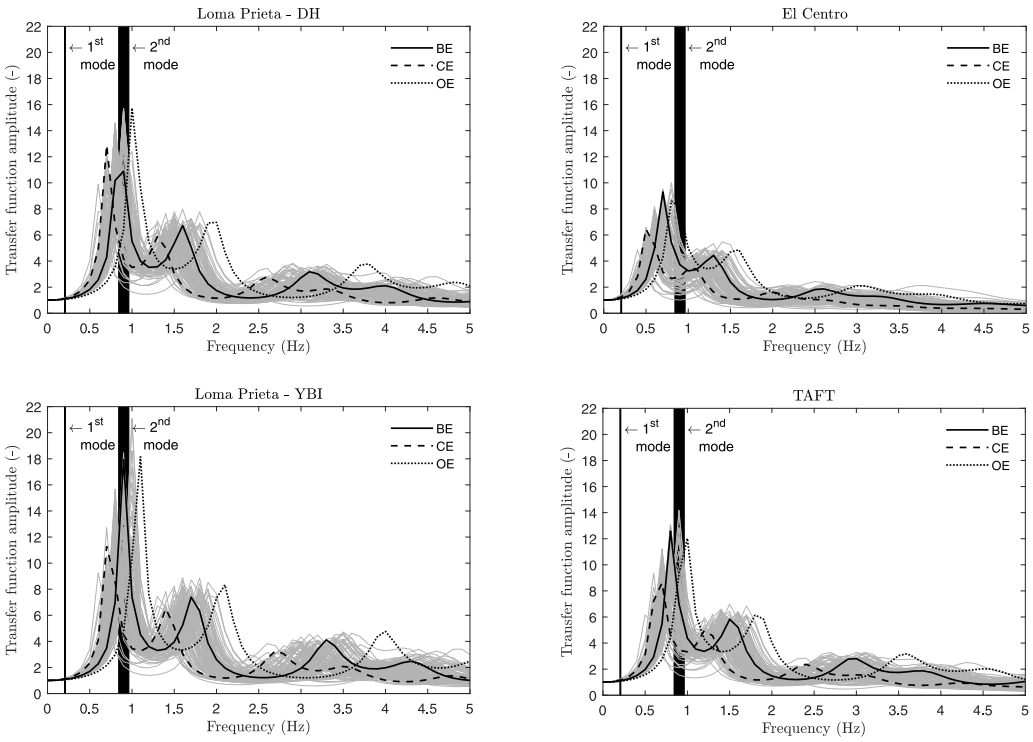

Fig. 7. Transfer functions from bedrock to mudline, per seismic motion, for all different soil profile input realizations. The values of the 1st and 2nd eigenmode ranges are presented in Table 5.

Fig. 8 illustrates the Response Spectra (in the form of spectral accelerations) at mudline for the four different earthquake motions at free-field. A damping value of 5% critical is assumed for the response spectrum. In all cases the high frequency content of the input seismic motions is de-amplified, while the low frequency components are amplified due to the local site effects.

At the high-frequency region of the spectra, i.e., above 0.8–1.2 Hz, the OE soil interpretation is consistently resulting in higher accelerations comparing to the BE and CE. This is because the OE soil profile corresponds to stiffer soil material, which is amplifying the higher frequency components of the input motion. The opposite phenomenon is observed at the low-frequency range, where the CE soil interpretation is governing the response. In all four seismic motions the response spectra show amplification of the spectral acceleration at the characteristic site frequency, being between 0.5 and 0.9 Hz, depending on the soil properties.

Despite the lower amplitude transfer functions of "El Centro", as discussed above, this is the seismic motion imposing the highest accelerations demand. In this seismic event, the 2nd eigenmode is located very close to the peak accelerations.

By comparing the relative location of the three distinct soil interpretation (BE, CE and OE) to the frequency range covered by the 2nd eigenmode, an indication about the most "critical" soil interpretation may be derived per seismic motion: "Loma Prieta - DH": CE; "EL Centro": BE and/or OE; "TAFT": BE and/or CE; "Loma Prieta - YBBI": CE.

Fig. 9 depicts the bending moment profiles over the height of the support structure (envelope of the maximum values at every level, for each time-domain calculation), normalized over the maximum bending moment in all considered simulations. This maximum occurs few meters below mudline for the "El Centro" earthquake. Note that LAT represent the zero reference level, in line with Table 4. The variation in the resulting seismic load is caused by the varying intensity of the seismic input motions (e.g., in terms of PGA), and the frequency content of the excitation in relation to the system's eigenfrequencies. As illustrated in Fig. 8, "El Centro"'s dominant frequency range, with the highest spectral acceleration at mudline, is very close to the system's 2nd eigenfrequency.

One important observation for all four seismic motions is that there is no single soil interpretation being the most demanding for the entire support structure. This is very clear in case of the "EL Centro" and the "TAFT" seismic motions, while for both "Loma Prieta" motions, the CE is mainly driving the loads apart from some small parts of the structure close to the mudline and the pile tip.

The observation of the most "critical" soil interpretation discussed above is verified. While for the two "Loma Prieta" motions the CE soil interpretation is mostly driving, and that could be predicted by the response spectra plots, this is not the case for the "El Centro" and the "TAFT" seismic motions. However, the response spectra correctly indicated which two out of the three distinct soil interpretations will cause the highest loads.

5. Discussion

In this Section the results of the numerical analyses are processed and presented in a format that could give some key insights for the engineering practice.

Fig. 10 illustrates the percentage probability of occurrence of each bin of the normalized bending moment. The same normalization as in Fig. 9 is adopted, while the limits and tick-marks of the horizontal axes vary per motion for better visualization. The results for three key components of the structure are presented, i.e., the main bearing, the tower top and the tower bottom (see Fig. 1).

All resulting load distributions are skewed despite the fact that the underlying distributions of the input soil parameters are normal (see Section 2.1). The mean load value (denoted by dotted lines) does not necessarily coincide with the most probable load (mode), but it is "biased" towards higher or lower load values. The 85-percentile (denoted by dashed lines) is always more conservative than the most probable load (mode). The 85-percentile load level has here been specifically chosen as a representative load level in accordance with the

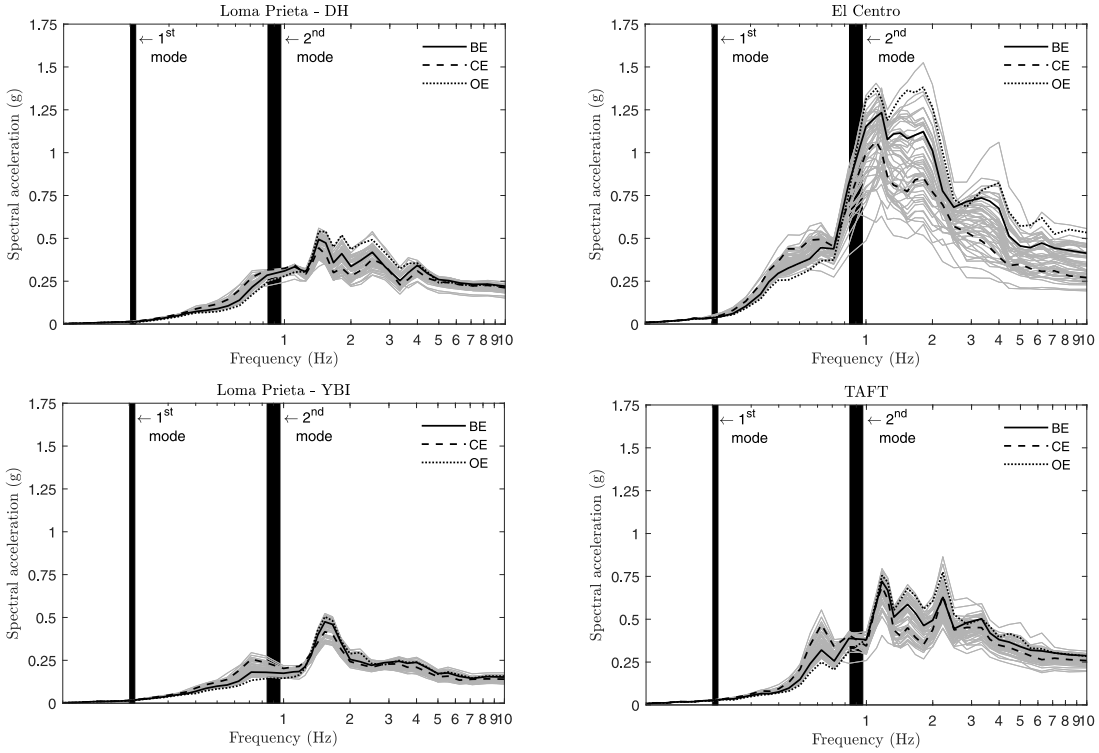

Fig. 8. Response spectra at mudline, per seismic motion, for all different soil profile input realizations. Damping is assumed to be 5%. The values of the 1st and 2nd eigenmode ranges are presented in Table 5.

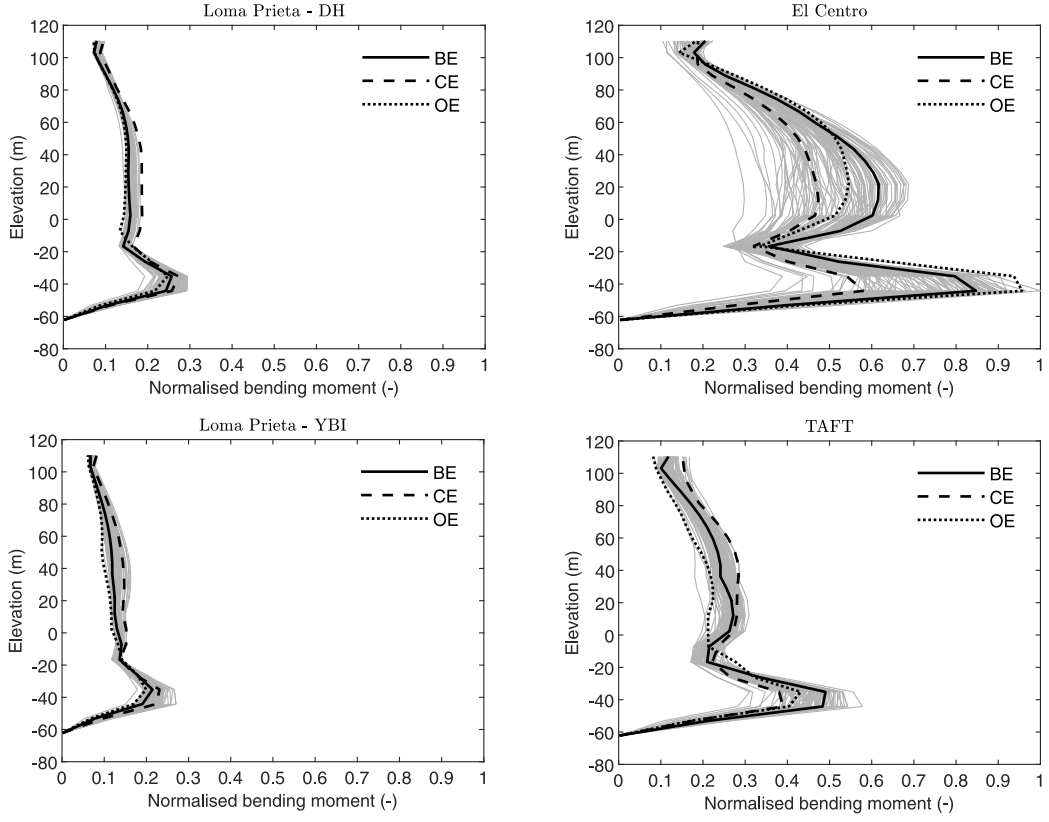

Fig. 9. Normalized bending moment distribution over height, per seismic motion, for all different soil profile input realizations.

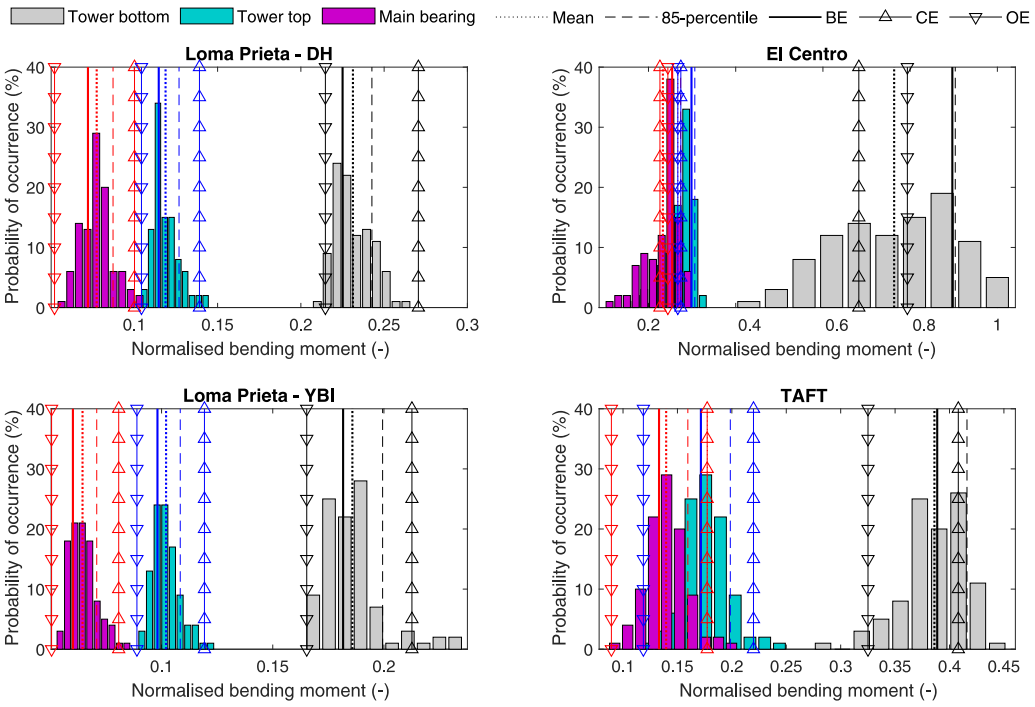

Fig. 10. Probability distribution of seismic loads at three elevations (main bearing, tower top and tower bottom). Results for the BE, CE and OE soil interpretations are presented together with the mean value and the 85-percentile of each distribution.

international standard for seismic evaluation of wind turbine support structures, IEC61400-6 (2020).

Simulations with the BE soil interpretation (denoted by solid lines) indicate that the corresponding BE loads can be close to the most probable load (e.g., "El Centro"), but they may also be non-conservative (e.g., "TAFT"). CE and OE soil interpretations are not necessarily "conservative" or "progressive" for the design against seismic loading. For instance, while CE appears to be very conservative for the "Loma Prieta" seismic motions, it is non-conservative for the component with the highest load, i.e., the tower bottom at the "El Centro" earthquake. In fact for this particular case, the CE load is lower than the OE load, and far lower than the most probable load (mode).

Interestingly, the two "Loma Prieta" seismic motions, which were originated from the same earthquake event but recorded at different location (see Section 2.2), have inherent characteristics which result in differences with respect to the computed transfer functions (Fig. 7) and bending moments at the three components of interest (Fig. 10). However, the probability distributions for both appear to have similar trends between the different soil interpretations.

To assess the severity of the resulting seismic loads a comparison with typical ULS load levels from environmental (hydrodynamic and aerodynamic) loading is attempted. The observations vary per component/elevation. At the tower bottom (22 mLAT; Table 4), the maximum seismic load of all analysed cases, caused by the "El Centro" seismic motion, corresponds to 70%–80% of the maximum ULS load at that elevation. At the tower top and the main bearing (about 113 mLAT; Table 4), the obtained seismic loads show big variation (see also Fig. 9) and tend to be rather close to the maximum ULS load at that elevation.

Fig. 11 presents the convergence of the 85-percentile normalized bending moment to within 5% load bounds, per seismic motion, at the three different components. As indicated by all figures, there is a minimum of about 15–20 simulations, i.e., different soil interpretations, in order to reach a convergence within 5% of the 85-percentile load. Additionally, note that the post-processed normalized bending moment may be higher than one (i.e., very conservative, higher than the max of all calculations), if only a small number of simulations is used (see Fig. 11, the "El Centro" seismic motion).

6. Conclusions and recommendations

The goal of this paper was to investigate the impact of geotechnical uncertainties on the seismic loading of OWT. The most insightful findings emerging from the results are summarized below. It is highlighted that the conclusions are related to the input conditions and assumptions of the presented case study. Nevertheless, similar outcome is expected for comparable cases. The reported conclusions are supported by SGRE's current experience in the seismic design of OWTs, aiming to inform the engineering community about the potential impact of typical uncertainties in the soil conditions to the seismic loading of OWTs.

- For the seismic design of OWTs it cannot be decided a priori which soil interpretation would result in a conservative or progressive design approach. For instance, the set of soil properties which would result to the most probable or the 85-percentile of the seismic load does not necessarily correspond to any of the BE, CE or OE soil interpretation sets. Thus, an increased number of realizations (soil profiles with different soil properties) needs to be considered for safe and sound designs. The exact number is considered to be project-specific, probably depending on the local site conditions, the wind turbine and support structure characteristics, but also on the applied seismic motions. The following pragmatic approach is recommended by the authors in order to mitigate this risk.
  - At least two different sets of soil properties are considered for the seismic design of OWTs under the selected project-specific input seismic motions.
  - The amplitude of the transfer functions at mudline can be used to identify the critical eigenmode which could resonate with the input seismic motion and lead to the highest seismic loads.
  - The response spectra at mudline (spectral accelerations) can be used to identify which set of soil parameters may generate the highest loads. However, this cannot be conclusive for the whole support structure (tower and foundation) and the RNA components.

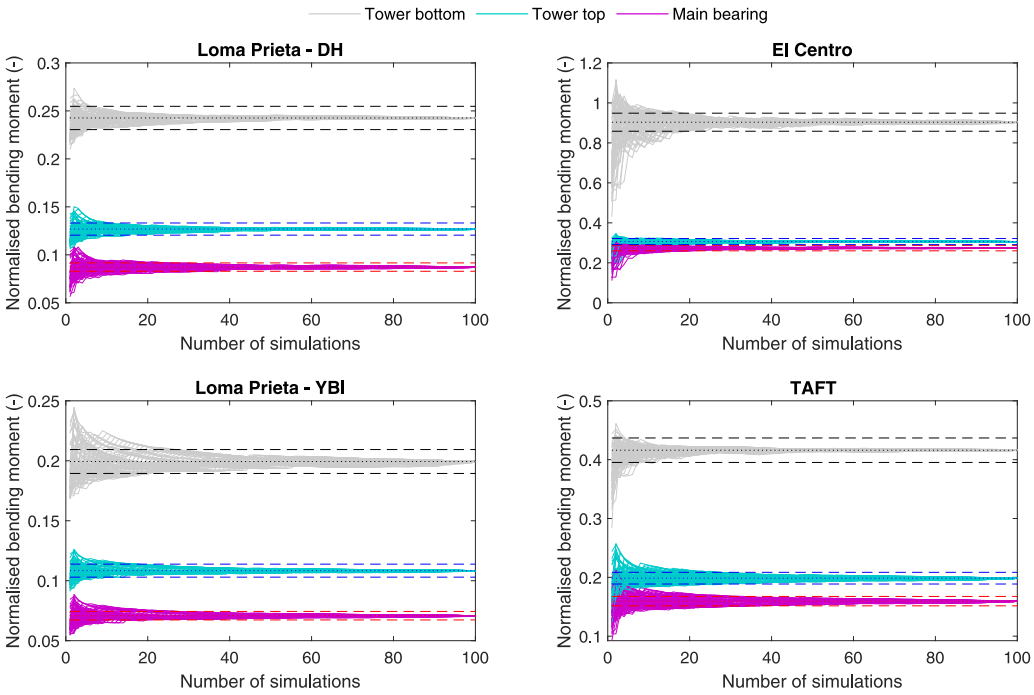

Fig. 11. Convergence of the 85-percentile normalized bending moment to within 5% load bounds, at three different elevations (main bearing, tower top and tower bottom).

  - A sensitivity study of the seismic response is advised if, at one or more elevations/components, the obtained seismic load is close to the ULS design load level, and, the variation of the seismic load (considering at least two different sets of soil properties) is wide. Exact values of proximity or span cannot be suggested. Engineering judgment is required for decision-making on a project-specific basis.

- For the analysis of the results, the 85-percentile value of the load distribution has been selected as a representative load level, following the recommendation of IEC61400-6 (2020), Annex O (informative). However, the obtained results indicated that the 85-percentile load level is, under the input conditions and assumptions of this study, always more conservative than the most likely load level of the distribution. As such, for greater accuracy and reduced over-conservatism, it may be required to consider a percentile lower than 85 as a representative load level for the seismic design of OWT.
- The plasticity index parameter of the clay layers, which is directly controlling the soil material hysteretic damping, has a significant effect on the transfer functions of the input seismic motion. Hence, this is an important material parameter to account for, and thorough evaluation via soil investigation is required. If a considerable amount of clay is present it is advised to either select this parameter on the conservative side or conduct a parametric study to evaluate its influence on the seismic loads.
- As a general note, well-planned and executed site investigation, together with advanced laboratory testing, could reduce the uncertainty related to the input soil parameters. Based on the results of this study, this is considered of high importance for the seismic prone regions, currently in the process of offshore wind development.

Based on the outcome of this study and its limitations, in relation to adopted assumptions, the following recommendations are suggested for follow-up research.

- The derived conclusions are based on one hundred different soil profile realization combined with four different earthquake motions. Employment of a higher number of soil profiles and motions would be needed in order to obtain more conclusive results.
- As discussed in Section 2.3 the equivalent linear method is used to derive seismic accelerations along depth via one-dimensional site response analyses. While this method is acceptable in engineering practice (under certain soil and seismic conditions), a non-linear approach is deemed necessary in order to examine a bigger variety of seismic motion intensities and soil stiffness.
- Moreover, an effective stress based non-linear method could be used to study the effects of pore pressure generation and dissipation during and after the seismic event. In this way the effect of soil uncertainties in combination with liquefaction on seismic design of OWT can be studied.
- The employment of non-linear soil reaction curves with controlled accumulation of lateral deflection under cyclic loading is advised to investigate the potential of permanent lateral deflection and/or rotation of the support structure under seismic and environmental loading.

CRediT authorship contribution statement

S. Panagoulias: Project administration, Conceptualization, Methodology, Software, Data curation, Interpretation of results, Visualization, Conclusions, Writing – original draft, Writing – review & editing. **C. de Winter:** Project administration, Conceptualization, Methodology, Software, Data curation, Interpretation of results, Visualization, Conclusions, Writing – original draft, Writing – review & editing. **S.T. Navalkar:** Conceptualization, Methodology, Data curation, Interpretation of results, Visualization, Conclusions, Writing – original draft, Writing – review & editing. **A. Nernheim:** Conceptualization, Methodology, Software, Data curation, Interpretation of results, Conclusions, Writing – review & editing.

Declaration of competing interest

The authors declare that they have no known competing financial interests or personal relationships that could have appeared to influence the work reported in this paper.

Data availability

The data that has been used is confidential.

References

ACE JIP, 2021. Alleviating cyclone and earthquake challenges for wind farms (ACE) joint industry project, led by det norske veritas (DNV). https://www.dnv.com/news/new-joint-industry-project-kicks-off-to-reduce-cyclone-and-earthquake-challenges-for-wind-turbines-164399 (accessed: 02.10.2022).

Alati, N., Failla, G., Arena, F., 2015. Seismic analysis of offshore wind turbines on bottom-fixed support structures. Phil. Trans. R. Soc. A 373 (2035), 20140086. http://dx.doi.org/10.1098/rsta.2014.0086.

Anastasopoulos, I., Theofilou, M., 2016. Hybrid foundation for offshore wind turbines: Environmental and seismic loading. Soil Dyn. Earthq. Eng. 80, 192–209. http://dx.doi.org/10.1016/j.soildyn.2015.10.015.

API, 2014. RP 2A-WSD - Recommended Practice for Planning, Designing and Constructing Fixed Offshore Platforms. American Petroleum Institute, Washington.

Ashford, S., Boulanger, R., Donahue, J., Stewart, J., 2011. Geotechnical Quick Report on the Kanto Plain Region during the March 11, 2011, Off Pacific Coast of Tohoku earthquake, Japan. Report No GEER-025a, Geotechnical Extreme Events Reconnaissance (GEER).

Bhattacharya, S., Amani, S., Prabhakaran, A., Macabuag, J., 2022. Hazard considerations in the vulnerability assessment of offshore wind farms in seismic zones. Earthq. Eng. Resil. 1 (1), 88–109. http://dx.doi.org/10.1002/eer2.11.

Bhattacharya, S., Biswal, S., Aleem, M., Amani, S., Prabhakaran, A., Prakhya, G., Lombardi, D., Mistry, H., 2021. Seismic design of offshore wind turbines: Good, bad and unknowns. Energies 14 (12), http://dx.doi.org/10.3390/en14123496.

Borcherdt, R., 1994. The Loma Prieta, California, Earthquake of October 17, 1989: Strong Ground Motion. US Government Printing Office Washington, DC, URL: https://pubs.usgs.gov/pp/pp1551/pp1551a/.

Byrne, B., Burd, H., Zdravkovic, L., Abadie, C., Houlsby, G., Jardine, R., Martin, C., McAdam, R., Pacheco Andrade, M., Pedro, A., Potts, D., Taborda, D., 2019. PISA design methods for offshore wind turbine monopiles. In: OTC - Offshore Technology Conference. http://dx.doi.org/10.4043/29373-MS.

Carswell, W., Arwade, S., DeGroot, D., Lackner, M., 2015. Soil-structure reliability of offshore wind turbine monopile foundations. Wind Energy 18 (3), 483–498. http://dx.doi.org/10.1002/we.1710.

DNV, 2021. Alleviating Cyclone and Earthquake Challenges for Wind farms (ACE) Joint Industry Project - Final Report Seismic Workstream. Unpublished Report - Distributed Among the ACE JIP Partners.

DNV-RP-0585, 2021. Recommended practice. In: Seismic Design of Wind Power Plants. Det Norske Veritas, ed. August 2021.

DNV-RP-C207, 2015. Recommended practice. In: Statistical Representation of Soil Data. ed. January 2015.

DNV-ST-0437, 2016. Standard. In: Loads and Site Conditions for Wind Turbines. Det Norske Veritas, ed. November 2016.

EduPro Civil Systems, I., 2020. ProShake ground response analysis program, version 2.0. http://www.proshake.com/index.html.

Gazetas, G., Mylonakis, G., Nikolaou, A., 1995. Simple methods for the seismic response of piles applied to soil-pile-bridge interaction. In: International Conferences on Recent Advances in Geotechnical Earthquake Engineering and Soil Dynamics, Vol. 13. URL: https://scholarsmine.mst.edu/icrageesd/03icrageesd/session16/13?utm_source=scholarsmine.mst.edu%2Ficrageesd%2F03icrageesd%2Fsession16%2F13&utm_medium=PDF&utm_campaign=PDFCoverPages.

Gelagoti, F., Kourkoulis, R., Georgiou, I., Karamanos, S., 2019. Soil–structure interaction effects in offshore wind support structures under seismic loading. J. Offshore Mech. Arct. Eng. 141 (6), http://dx.doi.org/10.1115/1.4043505.

Guntur, S., Jonkman, J., Sievers, R., Sprague, M.A., Schreck, S., Wang, Q., 2017. A validation and code-to-code verification of FAST for a megawatt-scale wind turbine with aeroelastically tailored blades. Wind Energy Sci. 2 (2), 443–468. http://dx.doi.org/10.5194/wes-2-443-2017.

GWEC, 2022. Global wind report 2022, global wind energy council. https://gwec.net/global-wind-report-2022/.

Hsu, Y., Lu, Y., Khoshnevisan, S., Juang, H., Hwang, J., 2022. Influence of geological uncertainty on the design of OWTF monopiles. Eng. Geol. 303, 106621. http://dx.doi.org/10.1016/j.enggeo.2022.106621.

Hussien, M., Karray, M., Tobita, T., Iai, S., 2015. Kinematic and inertial forces in pile foundations under seismic loading. Comput. Geotech. 69, 166–181. http://dx.doi.org/10.1016/j.compgeo.2015.05.011.

IEC61400-3, 2019. International Standard. Wind energy generation systems - Part 3-1: Design requirements for fixed offshore wind turbines. International Electrotechnical Commission, ed. April 2019.

IEC61400-6, 2020. International standard. In: Wind Energy Generation Systems - Part 6: Tower and Foundation Design Requirements. International Electrotechnical Commission, ed. April 2020.

Jeanjean, P., 2009. Re-assessment of P-Y curves for soft clays from centrifuge testing and finite element modeling. http://dx.doi.org/10.4043/20158-MS.

Katsanos, E., Thöns, S., Georgakis, C., 2016. Wind turbines and seismic hazard: A state-of-the-art review. Wind Energy 19, 2113–2133. http://dx.doi.org/10.1002/we.1968.

Kausel, E., 2010. Early history of soil–structure interaction. Soil Dyn. Earthq. Eng. 30 (9), 822–832. http://dx.doi.org/10.1016/j.soildyn.2009.11.001.

Kaynia, A., 2019. Seismic considerations in design of offshore wind turbines. Soil Dyn. Earthq. Eng. 124, 399–407. http://dx.doi.org/10.1016/j.soildyn.2018.04.038.

Kramer, S., 1996. Geotechnical Earthquake Engineering. Prentice Hall, Upper Saddle River, New Jersey, USA.

Liu, X., Lu, C., Li, G., Godbole, A., Chen, Y., 2017. Effects of aerodynamic damping on the tower load of offshore horizontal axis wind turbines. Appl. Energy 204, 1101–1114. http://dx.doi.org/10.1016/j.apenergy.2017.05.024.

MATLAB, 2018. version 9.5 (R2018b). The MathWorks Inc., Natick, Massachusetts.

Matlock, H., Foo, S., Bryant, M., 1978. Simulation of later pile behaviour under earthquake motion. In: Earthquake Engineering and Soil Dynamics: Proceedings of the ASCE Geotechnical Engineering Division Specialty Conference.

Medina, C., Aznárez, J., Padrón, L., Maeso, O., 2013. Effects of soil–structure interaction on the dynamic properties and seismic response of piled structures. Soil Dyn. Earthq. Eng. 53, 160–175. http://dx.doi.org/10.1016/j.soildyn.2013.07.004.

Mo, R., Cao, R., Liu, M., Li, M., Huang, Y., 2021. Seismic fragility analysis of monopile offshore wind turbines considering ground motion directionality. Ocean Eng. 235, 109414. http://dx.doi.org/10.1016/j.oceaneng.2021.109414.

Page, A., Grimstad, G., Eiksund, G., Jostad, H., 2018. A macro-element pile foundation model for integrated analyses of monopile-based offshore wind turbines. Ocean Eng. 167, 23–35. http://dx.doi.org/10.1016/j.oceaneng.2018.08.019.

Panagoulias, S., Nernheim, A., Lisi, D., Lahoz, M., Brinkgreve, R., 2020. Concept design study of laterally loaded monopiles in sand. In: 4th International Symposium on Frontiers in Offshore Geotechnics (Postponed). pp. 1312–1322, URL: https://www.isfog2020.org/.

Patra, S., Haldar, S., 2021. Seismic response of monopile supported offshore wind turbine in liquefiable soil. Structures 31, 248–265. http://dx.doi.org/10.1016/j.istruc.2021.01.095.

Patra, S., Haldar, S., Bhattacharya, S., 2022. Predicting tilting of monopile supported wind turbines during seismic liquefaction. Ocean Eng. 252, 111145. http://dx.doi.org/10.1016/j.oceaneng.2022.111145.

Pisanò, F., 2019. Input of advanced geotechnical modelling to the design of offshore wind turbine foundations. In: In Proc. XVII European Conference on Soil Mechanics and Geotechnical Engineering. http://dx.doi.org/10.32075/17ECSMGE-2019-1099.

Reale, C., Tott-Buswell, J., Prendergast, L.J., 2021. Impact of geotechnical uncertainty on the preliminary design of monopiles supporting offshore wind turbines. ASCE-ASME J. Risk Uncertain. Eng. Syst. B: Mech. Eng. 7 (4), http://dx.doi.org/10.1115/1.4051418.

Rubak, R., Petersen, J.T., 2005. Monopile as part of aeroelastic wind turbine simulation code. In: In Proc. Copenhagen Offshore Wind Denmark.

Seed, H., Idriss, I., 1970. Soil Moduli and Damping Factors for Dynamic Response Analyses. Earthquake Engineering Research Center, University of California, Berkeley.

Tran, T., Salman, K., Han, S., Kim, D., 2020. Probabilistic models for uncertainty quantification of soil properties on site response analysis. ASCE-ASME J. Risk Uncertain. Eng. Syst. A 6 (3), 04020030. http://dx.doi.org/10.1061/AJRUA6.0001079.

Valamanesh, V., Myers, A., 2014. Aerodynamic damping and seismic response of horizontal axis wind turbine towers. J. Struct. Eng. 140 (11), 04014090. http://dx.doi.org/10.1061/(ASCE)ST.1943-541X.0001018.

Vucetic, M., Dobry, R., 1991. Effect of soil plasticity on cyclic response. J. Geotech. Eng. ASCE 117, 89–107.

Wang, L., Ishihara, T., 2022. A semi-analytical one-dimensional model for offshore pile foundations considering effects of pile diameter and aspect ratio. Ocean Eng. 250, 110874. http://dx.doi.org/10.1016/j.oceaneng.2022.110874.

Xi, R., Wang, P., Du, X., Xu, C., 2021. Dynamic behaviors of wind turbines under wind and earthquake excitations. J. Renew. Sustain. Energy 13 (4), 043306. http://dx.doi.org/10.1063/5.0054746.

Xi, R., Xu, C., Du, X., Hesham El Naggar, M., Wang, P., Liu, L., Zhai, E., 2022. Framework for dynamic response analysis of monopile supported offshore wind turbine excited by combined wind-wave-earthquake loading. Ocean Eng. 247, 110743. http://dx.doi.org/10.1016/j.oceaneng.2022.110743.

Yeter, B., Garbatov, Y., Guedes Soares, C., 2019. Uncertainty analysis of soil-pile interactions of monopile offshore wind turbine support structures. Appl. Ocean Res. 82, 74–88. http://dx.doi.org/10.1016/j.apor.2018.10.014.

Zhang, J., Yuan, G., Zhu, S., Gu, Q., Ke, S., Lin, J., 2022. Seismic analysis of 10 MW offshore wind turbine with large-diameter monopile in consideration of seabed liquefaction. Energies 15, 7. http://dx.doi.org/10.3390/en15072539.